Available online at www.sciencedirect.com
ScienceDirect
Journal of Fluorine Chemistry 129 (2008) 210–216
JOURNAL OF FLUORINE CHEMISTRY
www.elsevier.com/locate/fluor

Syntheses and evaluation of fluorinated benzothiazole anilines as potential tracers for β-amyloid plaques in Alzheimer's disease

Ming-Qiang Zheng [a,b], Duan-Zhi Yin [a,*], Jin-Ping Qiao [c], Lan Zhang [a], Yong-Xian Wang [a]

[a] *Research Center of Radiopharmaceuticals, Shanghai Institute of Applied Physics, Chinese Academy of Sciences, Shanghai 201800, China*
[b] *Graduate School of the Chinese Academy of Sciences, 19 YuQuan Road, Beijing 100049, China*
[c] *Hefei National Laboratory for Physical Sciences at Microscale and Department of Neurobiology, School of Life Sciences, University of Science & Technology of China, Hefei, Anhui 230027, China*

Received 5 October 2007; received in revised form 5 November 2007; accepted 5 November 2007
Available online 17 November 2007

Abstract

[^{11}C]2-(4′-(Methylamino)phenyl)-6-hydroxybenzothiazole ([^{11}C]PIB) is a most potential PET tracer for detecting the β-amyloid plaques in Alzheimer's disease. Here the syntheses of three fluorinated PIB, namely 2-(4′-(methylamino)phenyl)-6-fluoroethoxybenzothiazole (*O*-FEt-PIB), 2-(4′-(methylamino)phenyl)-6-fluoro-benzothiazole (F-*N*-Me) and 2-(4′-(dimethylamino)phenyl)-6-fluorobenzo-thiazole (F-*N*,*N*-Me), and the radiosynthesis of one corresponding ^{18}F-labeled PIB compound, [^{18}F]*O*-FEt-PIB, as well as their in vitro/in vivo biological characters were reported. The structures of the products were confirmed by IR, ^{1}H NMR, EI/ESI-MS, elemental analysis and HRMS techniques. The radiolabeled product was characterized by radio-TLC and radio-HPLC and purified by semi-preparative radio-HPLC. The suitable biological characters showed these tracers were potential to be developed as probes for detecting β-amyloid plaques in Alzheimer's disease.
© 2007 Elsevier B.V. All rights reserved.

Keywords: Alzheimer's disease; F-*N*-Me; F-*N*,*N*-Me; [^{18}F]*O*-FEt-PIB; PET

1. Introduction

Alzheimer's disease (AD) is a neurodegenerative disease, with aggregates of β-amyloid (Aβ) peptides and neurofibrillary tangles in the brain. Positron emission tomography (PET) is a very useful and powerful technology to study human brain. PET imaging of AD has many aspects of significance for diagnostic and therapeutic developments. Small molecules for detecting the β-amyloid plaques and tangles as potential PET ligands have been well developed [1]. Among them, benzothiazole anilines (BTA; Fig. 1), such as [^{11}C]PIB, are the most potential tracers and have been used in clinical studies [2]. BTAs are derivatives of thioflavin-T which is an amyloid-binding dye. Thioflavin has been used as a pharmacophore for development of amyloid-binding compounds [3,4]. It is well known that introducing a fluorine atom to a compound will probably change its biological activities and pharmacological properties [5]. What is more, it is estimated that substitution of OH to fluorine at the 6-position of BTA will increase lipophilicity and binding affinity to β-amyloid plaques. The syntheses of fluorinated PIB analogues have been under investigation for many years owing to their characters as potential fluorescence, MRI or PET tracers for detecting amyloid in AD brain [6–8].

Considering the short half-life of carbon-11 (20.4 min), one kind of fluorine-18 (109.6 min)-labeled PIB, [^{18}F]PIB, was synthesized and showed excellent in vitro and ex vivo properties and might be as a viable lead candidate for in vivo human studies [9]. Another fluorine-18-labeled PIB, [^{18}F]FBTA (Fig. 2), was successfully synthesized and its characters were under investigation by autoradiography of human AD brain sections and micro-PET in a transgenic mouse [10]. Here we reported the convenient synthesis of two fluorine-contained BTA compounds, 2-(4′-(methylamino)phenyl)-6-fluorobenzo-thiazole (F-*N*-Me) and 2-(4′-(dimethylamino)phenyl)-6-fluorobenzo-thiazole (F-*N*,*N*-Me). Both of them showed higher binding affinity to β-amyloid in the AD human brain homogenate than PIB [11]. Fluorescence staining of AD human brain sections with F-*N*-Me and F-*N*,*N*-Me confirmed the specific binding to β-amyloid. The more interesting finding was that F-*N*-Me might also bind to tangles, which is similar to that

* Corresponding author. Fax: +86 21 59554696.
E-mail address: comingzeng@yahoo.com.cn (D.-Z. Yin).

0022-1139/$ – see front matter © 2007 Elsevier B.V. All rights reserved.
doi:10.1016/j.jfluchem.2007.11.005

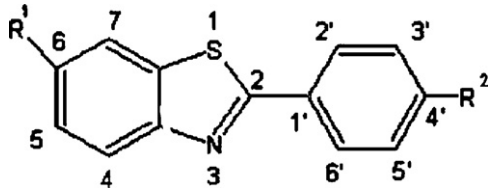

Fig. 1. Structure of 6-substituted benzothiazole anilines (BTA) derivatives [4].

of FDDNP [12]. Most recently, Stephenson et al. reported their excellent work about some fluoro-pegylated imaging agents as potential PET tracers for Aβ aggregates, which included the syntheses of similar structures ([^{18}F]5a–c) to [^{18}F]*O*-FEt-PIB and their distributions in normal mice [8]. Here we showed another radiosynthesis method of [^{18}F]*O*-FEt-PIB and its in vivo distribution in normal rats was also described. Because introducing a fluorine-18 atom into benzene ring directly without adjacent electron-withdrawing groups is almost impossible except the use of $^{18}F_2$, [^{18}F]F-*N*-Me and [^{18}F]F-*N*,*N*-Me are not synthesized and their application in MRI is under investigation.

2. Results and discussion

2.1. Synthesis of F-N-Me and F-N,N-Me

The synthesis is based on the following sequence of reactions as shown in Scheme 1. 5-Fluoro *o*-aminothiophenol (1) was prepared by base hydrolysis of the corresponding 2-amino-6-fluro-benzothiazole, then further reacted with commercially available *p*-(methylamino)-benzoic acid or (dimethylamino)-benzaldehyde to form the secondary (F-*N*-Me) or tertiary amine (F-*N*,*N*-Me) derivatives through different reaction routes. Fluorine atom is an electron-withdrawing group and this character is useful to increase the yield of condensing reactions comparing to the electron-donating group, for example, HO or EtO. Condition c is more convenient than b, either because of the short reaction time or the simpler procedure of the purification. But the raw compound *p*-(methylamino)-benzaldehyde is not commercial and estimated to be unstable.

2.2. Synthesis of O-FEt-PIB and [^{18}F]O-FEt-PIB

The preparation of *O*-FEt-PIB from 2-amimophenyl-6-ethoxybenzothiazole through four steps is shown in Scheme 2. The synthesis strategy was similar to that in ref. [4] with a fluoroethylate of PIB at the last step. It was estimated that the hydrogen at both NH and OH in PIB would be replaced by fluoroethyl group. However, when we used condition d, *O*-FEt-PIB was obtained as a main product. This interesting result made it possible that [^{18}F]fluoroethyltosylate ([^{18}F]FEtOTs) could selectively react with PIB in *O*-position with higher labeling yield and simpler purification procedure in certain conditions. [^{18}F]FEtOTs and [^{18}F]*O*-FEt-PIB were synthesized

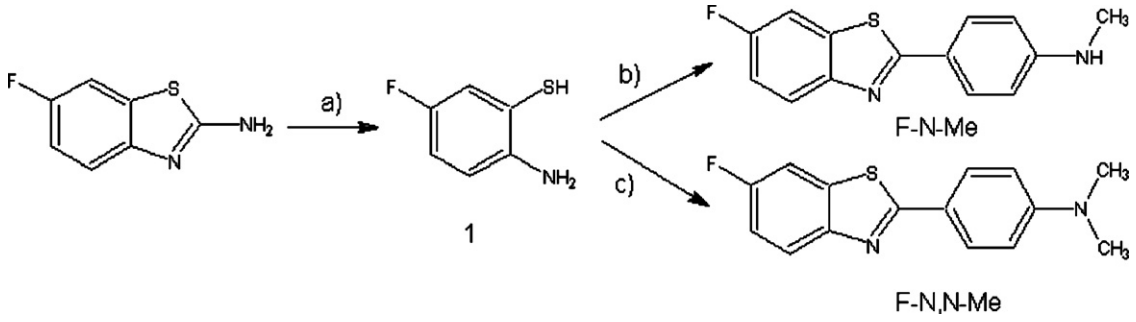

Scheme 1. Synthesis of 2-(4′-(methylamino)phenyl)-6-fluorobenzothiazole (F-*N*-Me) and 2-(4′-(dimethylamino)phenyl)-6-fluorobenzothiazole (F-*N*,*N*-Me). (a) Glycol, KOH, reflux for 48 h; (b) polyphosphoric acid. *p*-(Methylamino)-benzoic acid, 170 °C, 2 h; (c) Me_2SO, *p*-(dimethylamino)-benzaldehyde, 170 °C, 20 min.

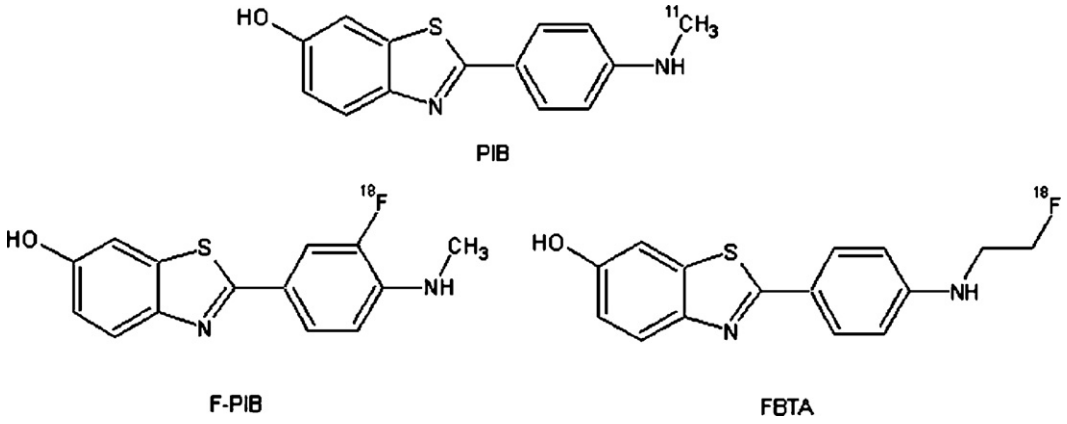

Fig. 2. Potential small molecular tracers for β-amyloid plaques [9,10].

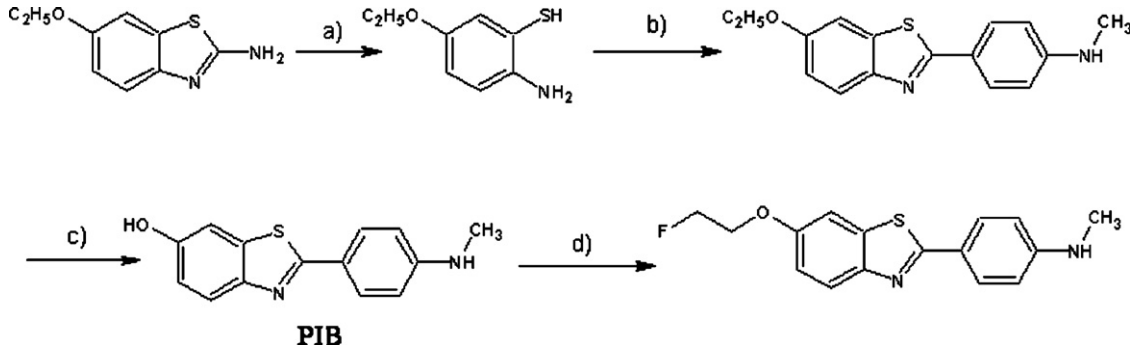

Scheme 2. Synthesis of 2-(4′-(dimethylamino)phenyl)-6-fluoroethoxybenzothiazole (*O*-FEt-PIB). (a) Glycol, KOH, reflux for 48 h; (b) polyphosphoric acid, *p*-(methylamino)-benzoic acid, 170 °C, 2 h; (c) 1 mol/L BBr_3/CH_2Cl_2 solution, 16 h; (d) DMF, 2-fluoroethyl tosylate, potassium iodide, potassium carbonate, 80 °C, 20 h.

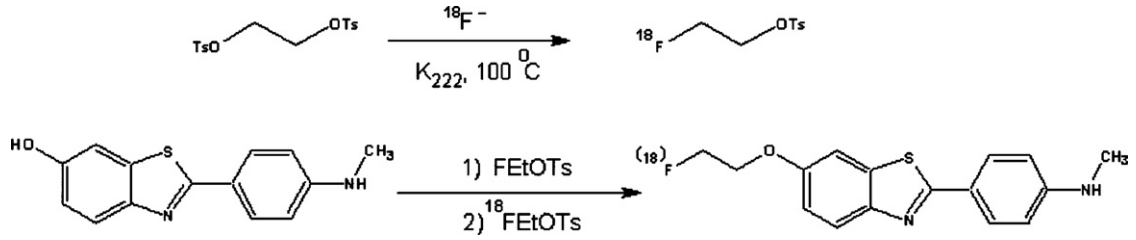

Scheme 3. Synthesis of [^{18}F]*O*-FEt-PD3. (1) DMF, KI, K_2CO_3, 80 °C, 20 h, (2) anhydrous CH_3CN, 110 °C, 20 min.

as shown in Scheme 3. The labeling yields were high (90 and 85%, respectively), but the total radiochemical yield of [^{18}F]*O*-FEt-PIB was only 5–10% (start from ^{18}F anion, total synthetic time of 95 min, decay not corrected). The reason was that only one quarter of the reaction-available [^{18}F]FEtOTs was obtained via the purification by C_{18} Sep-Park cartridge. The most of the lost was observed during the purification process through C_{18} Sep-Pak cartridge which was pre-saturated with water. The aimed product was identified by radio-TLC [$R_f = 0.16$ (reference 0.18) in $V_{hexane}/V_{ethyl\ acetate} = 4{:}1$]. Then the reaction products were purified by semi-preparative HPLC column (condition 1). The retention time of [^{18}F]*O*-FEt-PIB was about 14 min and well separated from other chemical species (for example, PIB, $t_R = 9.7$ min, [^{18}F]FEtOTs, $t_R = 11$ min and by-product, $t_R = 18$ min). The analytical HPLC condition (condition 2) and radio-TLC with two different conditions were used for quality control (RCP > 95%, $t_R = 18.2$ min (reference $t_R = 17.4$ min); $R_f = 0.66$ in $CHCl_3$ (reference $R_f = 0.62$) and 0.16 in *V*(hexane)/*V*(ethyl acetate) = 4:1 (reference $R_f = 0.18$)). Specific activity estimated by comparing UV peak intensity of purified [^{18}F]*O*-FEt-PIB and corresponding radioactivity was more than 740 TBq/mmol.

2.3. In vitro binding assay in human AD brain homogenate

Compounds F-*N*-Me, F-*N*,*N*-Me and *O*-FEt-PIB competed well with [^{3}H]PIB for binding to AD brain homogenate (Fig. 3). The K_i value for each compound was 0.20 (F-*N*-Me), 0.31 (F-*N*,*N*-Me) and 0.17 nM (*O*-FEt-PIB). In the same condition, K_i value of PIB was 1.59 nM. It confirmed the assumption that substitution of OH to an electron withdrawing group at the 6-position of BTA would increase its binding affinity to β-amyloid.

2.4. Fluorescent staining of senile plaques in human AD brain sections

To demonstrate the specific binding to Aβ plaques, the three compounds and thioflavin-T were used to stain paraffin sections of postmortem AD brain (Fig. 4). Like thioflavin-T, the staining of F-*N*-Me, F-*N*,*N*-Me or *O*-FEt-PIB was localized to Aβ plaques in the adjacent brain slices. The interesting results were that F-*N*,*N*-Me could either bind to amyloid plaques or cerebrovascular amyloid; F-*N*-Me could bind to both plaques and tangles. No distinct tangle-binding of F-*N*,*N*-Me was found. The identity of the plaques and tangles was confirmed by staining serial sections of the AD brain slices.

2.5. Biodistribution of [^{18}F]O-FEt-PIB in normal rats

Table 1 shows the brain, blood and bone entry of [^{18}F]*O*-FEt-PIB in normal Sprague–Dawley rats in terms of percent injected

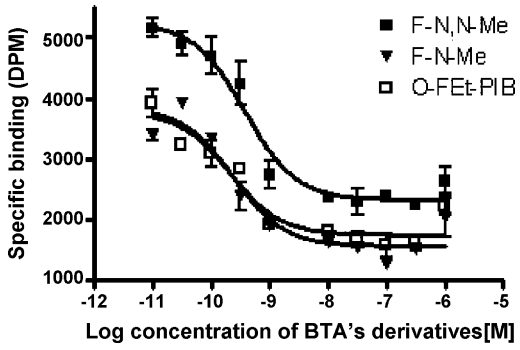

Fig. 3. Detennination of specific binding of BTA's derivatives in postmortem AD brain liomogenate. Each data point came from the average of four measurements and the bar represents the standard deviation (S.D.).

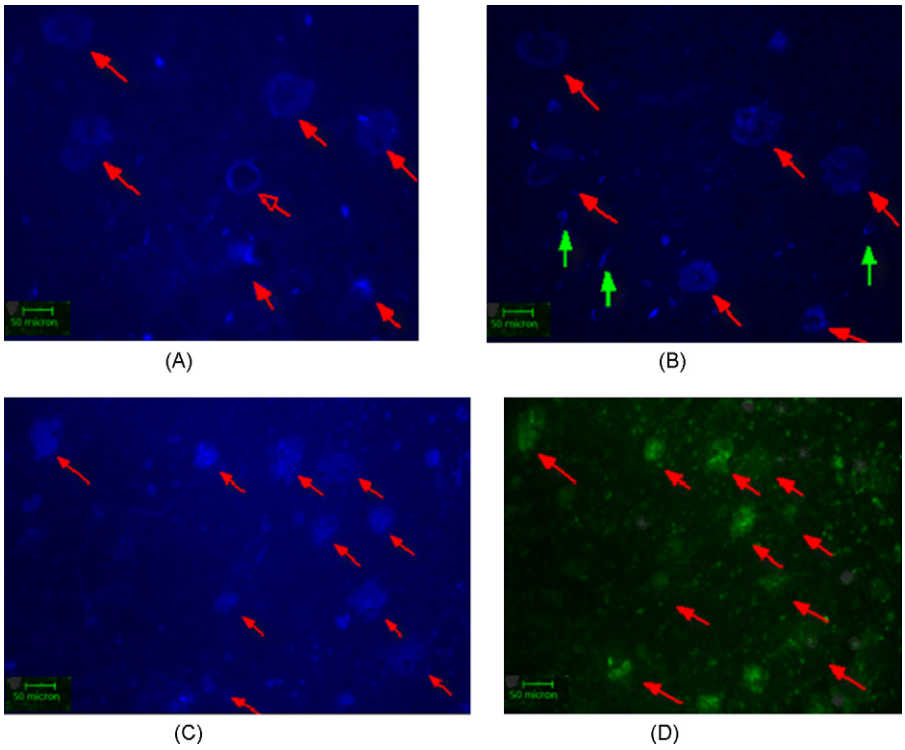

Fig. 4. Fluorescence micrographs of sections of AD brain (6 μm thick) stained with 1 μm F-*N*,*N*-Me (A), F-*N*-Me (B), *O*-FEt-PIB (C) and thioflavin-T (D). Section (A) shows F-*N*,*N*-Me could either stain plaques (marked by red arrows) or cerebrovascular amyloid (hollow arrows). Section (B) shows F-*N*-Me could either stain plaques (red arrows) or tangles (green arrows). Section (C and D) shows the corresponding plaques in adjacent AD brain slices. (For interpretation of the references to color in this figure legend, the reader is referred to the web version of the article.)

dose per gram of organ (%ID-kg)/g. The brains were divided into cortex, cerebrum (except cortex) and cerebellum. Organ entry (except bone) was high and quickly at early time after injection. The average (%ID-kg)/g value of [^{18}F]*O*-FEt-PIB in rat brains at 2 min p.i. was 0.5 and was good for a potential neuroreceptor radioligands. Among three parts of the brain, the uptake in cerebrum was a litter higher than that in cerebellum. The low uptake and radioactivity in bone indicates that no or little $^{18}F^{-}$ ion was generated while the metabolism. However, the clearance rate of radioactivity from brain tissues was slow, with a ratio value of about 2 comparing the radioactivity at 2–30 min. The ratio of brain radioactivity from 2 to 60 min was about 6 and this character was not as good as that of PIB (2–30 min ratio, 12 [4]).

Biodistribution studies in normal rats with 37 MBq [^{18}F]*O*-FEt-PIB at 5 min postinjection were performed (Table 2). Considering the slow clearance rate and rapid uptake of the tracer in brain, only one time point was chosen to evaluate the whole body distribution. It showed that the radioactivity in two parts of the brain did not distinguish from each other, and more radioactivities aggregated to cerebrum at 5 min (about 0.8) than at 2 min (about 0.6). Radioactivities were found mostly in liver and kidney, with 3.83 and 3.56, respectively. The muscle and bone were found the least amounts, with 0.48 and 0.39, individually. Comparing to the biodistribution of [^{18}F]5a in normal mice which was reported in ref. [8], the initial brain

Table 1
3B (brain, blood and bone) uptake and clearance of [^{18}F]*O*-FEt-PIB in normals rats at different time points after intravenous injection ((%ID-kg)/g, average of 3 rats ± S.D.)

Organ	2 mm	30 mm	60 mm	120 mm
Blood	1.79 ± 0.21	0.46 ± 0.15	0.20 ± 0.05	0.12 ± 0.05
Bone	0.21 ± 0.13	0.10 ± 0.04	0.09 ± 0.02	0.11 ± 0.03
Cerebel	0.50 ± 0.28	0.28 ± 0.16	0.08 ± 0.03	0.06 ± 0.03
Cortex	0.43 ± 0.25	0.18 ± 0.04	0.06 ± 0.02	0.04 ± 0.01
Cerebrum	0.64 ± 0.32	0.32 ± 0.22	0.09 ± 0.04	0.06 ± 0.02

Table 2
Biodistribntion of [^{18}F]*O*-FEt-PIB in normal rats ((%ID-kg)/g, $n = 5$, rats ± S.D.)

	5 min
Organ (body)	
Blood	1.40 ± 0.36
Muscle	0.48 ± 0.06
Lung	1.92 ± 0.89
Liver	3.83 ± 0.49
Kidney	3.56 ± 0.74
Spleen	1.25 ± 0.35
Heart	1.06 ± 0.19
Bone	0.39 ± 0.07
Organ (brain)	
Cerebellum	0.46 ± 0.04
Cortex (left)	0.43 ± 0.09
Cortex (right)	0.43 ± 0.21
Cerebrum (left)	0.81 ± 0.20
Cerebrum (right)	0.86 ± 0.27

uptake of [^{18}F]*O*-FEt-PIB in rats was less than that in mice (10.27% dose/g at 2 min postinjection), but the washout rate (rat, 2–60 min, 6) was faster than that in mice (2–60 min, 2.6). Another distinct difference existed in the bone uptake. The bone uptake in mice increased with time which indicated that in vivo defluorination was likely occurring. But in rats, no similar phenomenon was found.

3. Conclusion

Three fluorine-contained BTA compounds, F-*N*-Me, F-*N*,*N*-Me and *O*-FEt-PIB as well as [^{18}F]*O*-FEt-PIB was successfully synthesized. Binding assay showed that the binding affinity for each compound was higher than that of PIB. Fluorescent staining of senile plaques in human AD brain sections also showed the specific binding of these compounds to β-amyloid plaques. The interesting result was that F-*N*-Me could either bind to β-amyloid plaques or tangles. Another two compounds, F-*N*,*N*-Me and *O*-FEt-PIB, did not show this ability in our experiments. [^{18}F]*O*-FEt-PIB was synthesized via [^{18}F]FEtOTs as a fluoroethylated agent and the labeling yield was high (85%). The total synthetic time was 95 min with a radiochemical yield of 5–10% (start from ^{18}F anion, decay not corrected), and the specific activity was estimated more than 740 TBq/mmol. It was able to penetrate the blood–brain barrier and showed a high brain uptake ((ID%-kg)/g, 0.8 at 5 min p.i.) in rat, but the washout rate was a little slow (2–60 min ratio, 6). It was not observed that in vivo defluorination was occurring because the bone uptake was minimal and not increased with time. The in vivo evaluation of this tracer in AD model rats using micro-PET is underway in our laboratory.

4. Experimental

4.1. General experimental procedures

^{1}H NMR spectra was recorded on a Bruker AC-500 (500 MHz) instrument with Me_4Si as internal standards in the indicated solution described below. Chemical shifts were reported in δ values in parts per million (ppm) downfield from Me_4Si ($\delta = 0$) for proton NMR. Electron impact mass spectra (EI-MS) were obtained on MicroMass GCT CA 055 spectrometers. Infrared spectra (IR) were recorded on Avatar 370 FTIR (Thermo Nicolet) as KBr disc.

High-performance liquid chromatography (HPLC) was carried out on a Dionex system equipped with a P680 pump, a PDA-100 photodiode array detector and a NaI (Tl) scintillation detector. The columns used for identification and purification were LiChrosorb C_{18}, 10 μm, 300 mm × 3.9 mm and 300 mm × 7.8 mm, respectively. The column effluent passed through a UV (365 nm) detector and scintillation radioactivity detector in series. HPLC solvents consisted of CH_3OH (solvent A) and 0.1% CF_3COOH/H_2O (solvent B). HPLC gradient: 0–1 min 70% B, 1–25 min 20%, 25–40 min 20%. The flow rates of purification and analysis were 3 mL/min (condition 1, with column 300 mm × 7.8 mm) and 1 mL/min (condition 2, with column 300 mm × 3.9 mm), separately.

Radio-TLC analyse was performed using silica gel 60 GF-254 plates (Merck, Darmstadt, Germany) on a Bioscan system AR-2000 with Winscan software of Version 3.09. The radioactivity measurements were done using an automatic gamma counter (3-in. NaI (Tl) well crystal) coupled to a multichannel analyzer (SN682B).

All commercial reagents and solvents were used without further purification unless otherwise specified. 2-Amino-6-fluorobenzothiazole, 2-amino-ethoxybenzothiazole, *p*-(methylamino)-benzoic acid, *p*-(dimethylamino) benzaldehyde, 1,2-bis(tosylate)ethane and 2-fluoroethyl tosylate were purchased from Sigma–Aldrich Synthesis Ltd. (America) or Chemical Reagent Companies in Shanghai (China).

The animal experiments were performed in accordance with the ''Principles of Laboratory Animal Care'' (NIH Publication No. 86-23, revised 1985). Male and female Sprague–Dawley rats, weighing 400–500 g at the beginning of the experiment, were housed individually in a room maintained at 23 °C with a 12-h light:12-h dark cycle for the duration of the experiment.

4.2. Synthetic procedures

4.2.1. 2-Amino-5-fluorothiophenol (1)

The synthetic procedure was similar to that of 2-amino-5-methoxythiophenol in ref. [4], with a yield of 50.1%. ^{1}H NMR (acetone-d_6, 500 MHz), 6.81 (dd, $J_1 = 9$ Hz, $J_2 = 2.5$ Hz, 1H, H–4C), 6.56 (*t*, $J_1 = 8.5$ Hz, $J_2 = 2.5$ Hz, 2H, H–6C and H–3C); IR (KBr)ν: 3427, 2560, 1615, 1487, 1406, 1289, 1200, 1141, 864, 812, 685, 462 cm^{-1}; MS (*m*/*z*) (%) calcd. for C_6H_6NSF 143, found 142 (100), 98 (37). Anal. calcd. for C_6H_6FNS: C 50.33, H 4.22, F 13.27, N 9.78, S 22.39; found C 50.51, H 4.82, N 9.26, S 22.17.

4.2.2. 2-(4′-(Methylamino)phenyl)-6-fluorobenzothiazole (F-N-Me)

2-Amino-5-fluorothiophenol (0.72 g, 5.0 mmol) and 4-methylaminobenzoic acid (0.80 g, 5.0 mmol) were mixed together with PPA (polyphosphoric acid, ∼1 g) and heated to 170 °C under N_2 atmosphere with a mechanical mill for 1.5 h. The reaction mixture was cooled to room temperature and poured into 10% K_2CO_3 solution. Ethyl acetate (100 mL) was added to extract the organic compounds. The organic layer was separated, and the aq. layer was extracted with another 60 mL ethyl acetate (three times). All the organic layers were combined and washed with water. Evaporation of the solvent, the residue was first purified by flash column (hexanes:ethyl acetate = 4:1), then purified by recrystallization from THF/water to give 0.28 g (21.6%) 2-(4′-(methyl-amino)phenyl)-6-fluorobenzo thiazole as yellow needle crystal. ^{1}H NMR ($CDCl_3$, 500 MHz), 7.84 (s, 2H, H–2′C and H–3′C), 7.44 (dd, $J_1 = 9.0$ Hz, $J_2 = 2.5$ Hz, 2H, H–5′C and H–6′C), 7.10 (t, $J_1 = 8.5$ Hz, $J_2 = 2.5$ Hz, 1H, H–5C), 6.68 (d, $J = 8.5$ Hz, 2H, H–7C and H–4C), 2.81 (s, 3H, H–CH_3); IR (KBr)ν: 3312, 3273, 3289, 1605, 1564, 1480, 1450, 1276, 1250, 1062, 1049, 1001, 902, 854; MS (%): 258 (100). HRMS calcd. for $C_{14}H_{11}FN_2S$ 258.0627, found 258.0631.

4.2.3. 2-(4′-(Dimethylamino)phenyl)-6-fluorobenzothiazole (F-N,N-Me)

A mixture of 2-amino-5-fluorothiophenol (760 mg, 5.3 mmol) and 4-(dimethylamino) benzaldehyde (799 mg, 5.4 mmol) in Me_2SO (5 mL) was heated to 170 °C for 20 min. The reaction mixture was cooled to room temperature and poured into water. The organic component was extracted with ethyl acetate (2 × 30 mL). The combined organic layers were washed with water and dried over $MgSO_4$. Evaporation of the solvent, the residue was then purified by flash column (hexanes:ethyl acetate = 4:1) to give 373 mg (26%) yellow solid. ^{1}H NMR (acetone-d_6, 500 MHz), δ: 7.88 (d, J = 8.9 Hz, 2H, H–2′C and H–3′C), 7.50 (dd, J_1 = 8.5 Hz, J_2 = 2.5 Hz, 2H, H–5′C and H–6′C), 7.04 (dd, J_1 = 9.0 Hz, J_2 = 2.5 Hz, 8.9, 2.5 Hz, 1H, H–5C), 6.80 (s, 2H, H–7C and H–4C), 3.05 (d, J = 9.0 Hz, 6H, H–CH_3); IR (KBr)ν: 3447, 2972, 2917, 1607, 1489, 1455, 1365, 1222, 1166, 1065, 936, 819, 593 cm^{-1}; MS (%): 272 (100), 256 (13). HRMS calcd. for $C_{15}H_{23}FN_2S$ 272.0783, found 272.0781.

4.2.4. 2-(4′-(Methylamino)phenyl)-6-hydroxybenzothiazole (PIB compound)

The synthetic process was similar to that in ref. [4], with a yield of 60% as yellow solid. ^{1}H NMR ($CDCl_3$, 500 MHz), 7.81 (d, J = 8.5 Hz, 2H), 7.70 (d, J = 9.0 Hz, 1H), 7.36 (s, 1H), 6.98 (d, J = 9.3 Hz, 1H), 7.0 (d, J = 8.6 Hz, 2H), 2.87 (d, J = 5.5 Hz, 3H); IR (KBr)ν: 3395, 2870, 2786, 2665, 1609, 1577, 1494, 1428, 1340, 1279, 1241, 1180, 818 cm^{-1}; MS (m/z) (%) calcd. for $C_{14}H_{12}N_2OS$ 256, found 256 (100), 241 (11).

4.2.5. 2-(4′-(Methylamino)phenyl)-6-fluoroethoxybenzothiazole (O-FEt-PIB)

2-(4′-(Methylamino)phenyl)-6-hydroxybenzothiazole (PIB, 103 mg, 0.4 mmol), anhydrous potassium carbonate (55.4 mg, 0.4 mmol) and potassium iodide (61 mg, 0.37 mmol) were dissolved in DMF (10 mL), mixed with a magnetic stirer and heated to 80 °C. 2-Fluoroethyl tosylate (148 mg, 0.6 mmol) which dissolved in another 30 mL DMF was dropped into the mixture and then reacted for 20 h at 80 °C. Stopped the reaction, filtered the solvent while hot, evaporated the filtrate under reduced pressure and added water to remove the inorganic salt. Then the residue was filtered, rinsed with water, rinsed with ethanol and finally gave a brown solid. Purification by flash column (silica gel, hexanes:ethyl acetate = 4:1) to give 21 mg yellow solid. Analytical HPLC: condition 2, t_R = 17.4 min, purity 98% ^{1}H NMR ($CDCl_3$, 500 MHz), 8.21 (d, J = 8.5 Hz, 2H, H–ArCH_2), 8.12 (d, J = 9.0 Hz, 1H, H–5C), 7.38 (d, J = 8.5 Hz, 1H, H–5′C), 7.34 (d, J = 9.3 Hz, 1H, H–6′C), 7.18 (dd, J_1 = 8.6 Hz, J_2 = 2.5 Hz, 2H, H–2′C and H–3′C), 6.80 (s, 2H, H–7C and H–4C), 4.75 (dd, J_1 = 9.0 Hz, J_2 = 5.5 Hz, 2H, H–FCH_2), 3.40 (s, 3H, H–CH_3); IR (KBr)ν: 3443, 3265, 2958, 2924, 1744, 1720, 1609, 1561, 1543, 1489, 1460, 1446, 1333, 1261, 1227, 1208, 1181, 1083, 1021, 964, 940, 876, 802 cm^{-1}; MS (m/z) (%) calcd. for $C_{16}H_{15}FN_2OS$ 302, found 302 (42), 255 (100), 227 (16), 95 (23). HRMS calcd. for $C_{16}H_{15}FN_2OS$ 302.0889, found 302.0887.

4.2.6. Synthesis of 2-^{18}F-fluoroethyl tosylate ([^{18}F]FEtOTs)

[^{18}F]Fluoride, which produced by a cyclotron using ^{18}O(p, n)^{18}F reaction, was passed through a Sep-Pak Light QMA cartridge as an aq. solution in [^{18}O]-enriched water. The cartridge was dried by airflow, and the ^{18}F activity was eluted with 1 mL of Kryptofix 222/K_2CO_3 solution (10 mg of K_{222} and 2 mg of K_2CO_3 in CH_3CN/H_2O, v/v = 3.54/0.46). The solvent was then removed at 100 °C and the residue was azeotropically dried with 400 μL of CH_3CN three times under the nitrogen stream. A solution of 1,2-bis(tosylate)ethane (6–8 mg) in anhydrous CH_3CN (400 μL) was added to the reaction vessel which contained the dried ^{18}F fluoride. The mixture was heated at 110 °C for 10 min and the products were analyzed on radio-TLC. The R_f value was identical with that of the reference compound 2-fluoroethyl tosylate.

4.2.7. Synthesis of [^{18}F]O-FEt-PIB

After condensing the solution of [^{18}F]FEtOTs to about 20 μL, 2 mL of water was added and the mixture was pushed through a pre-saturated C_{18} Sep-Pak cartridge. The cartridge was dried under a nitrogen stream, and then rinsed with 2 × 1 mL ethyl acetate. The combined organic solution was collected to a reaction vessel and dried under a nitrogen stream with gentle heating (about 60 °C). PIB (3 mg) in 200 μL Me_2SO, 1 mol/L K_2CO_3 solution (20 μL) and CH_3CN (400 μL) were added to the vessel and heated for 20 min at 110 °C. The products were analyzed by radio-TLC and radio-HPLC, and then purified using semi-preparative HPLC Column (condition 1). Collected the elution from 13 to 15 min and dried at 60 °C under a nitrogen stream.

4.2.8. In vitro binding assays with AD brain homogenates

The AD human brain homogenates 3.21 ± 0.04 μg in the final mixture, 100 μL) were obtained through National Institute of Mental Health, National Institute of Health as an aqueous solutions protected in dry ice, which were homogenated again before use. The procedure was similar to that described in ref. [13] with some modification. The binding was assayed in 12 mm × 75 mm borosilicate glass tubes for saturation studies, with the mixture contained 100 μL homogenates and 10–350 μL [^{3}H]PIB (4.00×10^{-2} μCi/100 μL; 350, 250, 200, 150, 100, 80, 60, 40, 20, 10 μL) and adding PBS (pH 7.4) to a final volume of 1 mL. Nonspecific binding was defined in the presence of 50 μL PIB (1×10^{-3}mol/L in PBS) in five different tubes. For the competition binding, 10^{-4} to 10^{-9} mol/L compounds and 4.00×10^{-2} μCi [^{3}H]PIB were used for the studies. The mixture was incubated at 37 °C for 2 h. The radioactivity was counted next day in the scintillation counter (Beckman) with 57% counting efficiency. Under the assay conditions, the specifically bound fraction was less than 15% of the total radioactivity.

4.2.9. Fluorescent staining of senile plaques in human AD brain sections

Postmortem brain tissues from AD cases were obtained through Hefei National Laboratory for Physical Sciences at

Microscale and Department of Neurobiology, School of Life Sciences, University of Science & Technology of China, (from the Netherlands Brain Bank (Coordinator Dr I. Huitinga)). 6 μm thick serial sections of paraffin embedded blocks from the hippocampus were used for staining. Tissue was processed for staining and the staining protocols were following that in ref. [4]. Quenched tissue sections were taken from PBS (pH 7.4) into a solution of 1 μM F-*N*-Me, F-*N*,*N*-Me, thioflavin-T or *O*-FEt-PIB in PBS for 30 min. Fluorescent sections were viewed using a BX50 fluoromicroscope with an M-3204C CCD camera (Olympus, Tokyo) equipped with a B-filter/FITC (excites 360–460 nm).

4.2.10. Biodistribution in normal rats of [^{18}F]O-FEt-PIB

3B uptake and clearance studies were performed in male or female Sprague–Dawley rats, weighing 400–500 g (∼3 months old). The animal studies were performed according to the practice for the care and use of animals. Under pentabarbiturate anesthesia, each animal was weighed and received approximately 7.4 MBq (200 μCi) of [^{18}F]*O*-FEt-PIB through a lateral tail vein. The animals were killed by cardiac excision following cardiac puncture to obtain arterial blood samples and decapitation to obtain brain and crania at 2, 30, 60 and 120 min postinjection. The brains were rapidly excised and divided into cerebellum, cortex and cerebrum. All the samples were weighed and counted, and the counts were decay-corrected to the time of injection relative to ^{18}F standards (prepared from the injection solution). The tissue radioactivity was determined as percentage injected dose per gram tissue normalized to body weight (in kg) or (%ID-kg)/g.

For the biodistribution studies, each animal received approximately 37 MBq (1 mCi) of [^{18}F]*O*-FEt-PIB in 100 μL of 0.9% NaCl solution through a lateral tail vein under pentabarbiturate anesthesia. Rats (n = 5) were sacrificed by cervical dislocation. At 5 min postinjection, organs of interest were removed, weighed and counted. The data were acquired as the same method described above.

Acknowledgements

The authors will thank for the Amersham Kexing Pharmaceuticals Co. Ltd. for supplying us No-carrier-added [^{18}F]F$^-$ solution. This project was supported by the Science Foundation of Shanghai (No. 06DZ19506) and National Natural Science Foundation of China (No. 20601028).

References

[1] L.-S. Cai, R.B. Innis, V.W. Pike, Curr. Med. Chem. 14 (2007) 19–52.
[2] A. Nordberg, Lancet Neurol. 3 (2004) 519–527.
[3] C.A. Mathis, D.P. Holt, Y. Wang, G.F. Huang, M.L. Debnath, W.E. Klunk, Soc. Nucl. Med. (2002) (Abstract No. 605).
[4] C.A. Mathis, Y. Wang, D.P. Holt, G.F. Huang, M.L. Debnath, W.E. Klunk, J. Med. Chem. 46 (2003) 2740–2754.
[5] H.J. Borhm, D. Banner, S. Bendels, M. Kansy, B. Kuhn, K. Murler, U. Obst-Sander, M. Stahl, Chem. Biol. Chem. 5 (2004) 637–643.
[6] B.J. Bacskai, G.A. Hickey, J. Skoch, S.T. Kajdasz, Y. Wang, G.-F. Huang, C.A. Mathis, W.E. Klunk, B.T. Hyman, PNAS 100 (2003) 12462–12467.
[7] K. Noda-Saita, A. Yoneyama, Y. Shitaka, Y. Hirai, K. Terai, J. Wu, T. Takeda, K. Hyoda, N. Osakabe, T. Yamaguchi, M. Okada, Neuroscience 138 (2006) 1205–1213.
[8] K.A. Stephenson, R. Chandra, Z.-P. Zhuang, C. Hou, S. Oya, M.-P. Kung, H.F. Kung, Bioconjugate Chem. 18 (2007) 238–246.
[9] N.S. Mason, W.E. Klunk, M. Debnath, N. Flatt, G. Huang, L. Shao, C.A. Mathis, J. Label. Compd. Radiopharm. 50 (Suppl. 1) (2007) S87.
[10] U. Berndt, C. Stanetty, M. Berger, H. Kvaternik, T. Wolf, C. Kuntner, T. Wanek, P. Angelberger, C. Noe, J. Label. Compd. Radiopharm. 50 (Suppl. 1) (2007) S86.
[11] M.-Q. Zheng, D.-Z. Yin, L. Zhang, D.-F. Cheng, Y.-X. Wang, H.-C. Cai, J. Label. Compd. Radiopharm. 50 (Suppl. 1) (2007) S401.
[12] E.D. Agdeppa, V. Kepe, J. Liu, S. Flores-Torres, N. Satyamurthy, A. Petric, G.M. Cole, G.W. Small, S.-C. Huang, J.R. Barrio, J. Neurosci. 21 (2001) 1–5.
[13] L.S. Cai, F.T. Chin, V.W. Pike, H. Toyama, J.S. Liow, S.S. Zoghbi, K. Modell, E. Briard, H.U. Shetty, K. Sinclair, S. Donohue, D. Tipre, M.P. Kung, C. Dagostin, D.A. Widdowson, M. Green, W. Gao, M.M. Herman, M. Ichise, R.B. Innis, J. Med. Chem. 47 (2004) 2208–2218.